Limitations of electron spin resonance spectroscopy in assessing the role of free radicals in the thermal reactions of coal

ARTICLE *in* ENERGY & FUELS · JULY 1989

Impact Factor: 2.79 · DOI: 10.1021/ef00016a015

3 AUTHORS, INCLUDING:

Keith Bartle
University of Leeds
491 PUBLICATIONS **9,342** CITATIONS
SEE PROFILE

R. Kandiyoti
Imperial College London
312 PUBLICATIONS **6,264** CITATIONS
SEE PROFILE

diffusion resistance. In regime C (Figure 13c), the intermediate temperature region where $T \sim T_d$, $CaSO_4(s)$ (in addition to CaO(s)) forms initially to cause diffusional limitations but decomposes during some transition period since the temperature is high enough. This decomposition may also be enhanced by crack formation in the CaO(s) product layer,[21] which may increase $SO_2(g)$ diffusion rates out of the particle. The $CaSO_4(s)$ product layer thins and diffuses outward until, in the later period, $CaSO_4(s)$ decomposition is complete and CaO(s) is the sole oxidation product. This formation–decomposition sequence qualitatively explains the S-shaped $x - t$ curves in this regime.

Acknowledgment. This research was funded by the MIT-Exxon Combustion Research Program. Patient technical assistance from Anthony Modestino and assistance with the analytical techniques from Nancy Noftle are gratefully acknowledged.

Registry No. CaS, 20548-54-3; $CaSO_4$, 7778-18-9; CaO, 1305-78-8; SO_2, 12624-32-7.

Limitations of Electron Spin Resonance Spectroscopy in Assessing the Role of Free Radicals in the Thermal Reactions of Coal

Timothy G. Fowler† and Keith D. Bartle

School of Chemistry, University of Leeds, Leeds LS2 9JT, U.K.

Rafael Kandiyoti*

Department of Chemical Engineering and Chemical Technology, Imperial College, London SW7 2BY, U.K.

Received January 9, 1989. Revised Manuscript Received May 2, 1989

Numerous investigations based on electron spin resonance spectroscopy have reported observing changes in coal free-radical concentrations during pyrolysis and liquefaction. These observations constitute the main direct evidence for free-radical reactions that are thought to occur in coal during thermal treatment. As always, conclusions drawn from experimental observations depend critically on understanding exactly what parameter has been observed and on whether the observation has been carried out in a correct and physically significant manner. This report summarizes some recent findings pertaining to the interpretation of free-radical concentrations measured during in situ ESR–pyrolysis experiments and discusses the relationship between measured spin concentrations and the pyrolytic reactions of coal. A simple coal thermal breakdown model and numerical estimates are used to support the main conclusion that the concentration of reactive free radicals (which act as reaction intermediates) is too low to be measured with ESR and that observed changes in spin concentrations are due to relatively stable char free radicals.

Introduction

Recently, considerable interest has been expressed in free-radical reactions pertaining to the pyrolysis and liquefaction of coals and related model compounds and polymers.[1-5] Efforts at establishing likely reaction pathways[2] and estimation of kinetic parameters[4] for such reactions has proceeded in parallel with experimental studies making use mainly of electron spin resonance spectroscopy (ESR). The latter technique serves to either directly observe free radicals in situ, i.e., as heating of the substrate is in progress, or directly observe free radicals after the treated sample has been cooled down to ambient temperature, usually subsequent to removal from the reactor. Clear evidence of changes in concentrations of coal free radicals, as measured by ESR, when a sample of coal is subjected to thermal treatment has emerged from numerous investigations (e.g., see ref 3 and 6–8). These observations constitute the main direct evidence for free-radical reactions in coal pyrolysis. It is the relationship between the free radicals observed by ESR and the pyrolytic reactions of coal that is the subject of this paper.

Recently we have reported on in situ ESR measurements[9-16] for coals pyrolyzed in cells of variable geometry:

†Present address: British Gas PLC, Midlands Research Station, Wharf Lane, Solihull B91 2JW, U.K.

(1) Bockrath, B. C. In *Coal Science, II*; Gorbaty, M. L., Larsen, J. W., Wender, I., Eds.; Academic Press: New York, 1983; p 65.
(2) Stein, S. E. In *Chemistry of Coal Conversion*; Schlosberg, R. H., Ed.; Plenum: New York and London, 1985; p 13.
(3) Petrakis, L.; Grandy, D. W. *Free Radicals in Coals and Synthetic Fuels*; Elsevier: Amsterdam, 1983.
(4) Gavalas, G. R. *Coal Pyrolysis*; Elsevier: Amsterdam, 1982.
(5) Lewis, I. C.; Singer, L. S. In *Chemistry and Physics of Carbon*; Walker, P. L., Thrower, P. A., Eds.; Marcel Dekker: New York and Basel, 1981, Vol. 17, p 1.
(6) Smidt, J.; van Krevelen, D. W. *Fuel* **1959**, *38*, 355.
(7) Ladner, W. R.; Wheatley, R. *Br. Coal Util. Res. Assoc., Mon. Bull.* **1965**, *29*, 201.
(8) Sprecher, R. F.; Retcofsky, H. L. *Fuel* **1983**, *62*, 473.
(9) Fowler, T. G.; Kandiyoti, R.; Bartle, K. D. *Fuel* **1988**, *67*, 1711.
(10) Fowler, T. G.; Bartle, K. D.; Kandiyoti, R. *Fuel* **1987**, *66*, 1407.
(11) Fowler, T. G.; Bartle, K. D.; Kandiyoti, R. *Carbon* **1987**, *25*, 709.
(12) Fowler, T. G.; Bartle, K. D.; Kandiyoti, R. *Fuel* **1988**, *67*, 173.

0887-0624/89/2503-0515$01.50/0

a conventional closed tube cell, where the sample is sealed in an evacuated quartz tube, and a set of open cells, where the sample is located on a silica sinter while being continuously evacuated (vacuum cell) or swept with inert gas at variable flow rates (flow cell). The following are the main conclusions arising from this work:

a. Measurements of the temperature dependence of the ESR signal indicate that the Curie law, assumed in calculations of free-radical concentrations,[3,17] is generally poorly obeyed by samples pyrolyzed in sealed tubes.[11,14,15] However, when the pyrolysis is performed in an open cell, considerably better agreement with the Curie law is observed,[11,14,15] suggesting that more reliance may be placed on measurements performed with the open (flow or vacuum) cell geometry. The results were interpreted to indicate that, in sealed tubes, pyrolysis volatiles are in equilibrium with the free radicals of the residual char and that the position of this equilibrium is dependent on the temperature[14] of the cell, as well as the peak temperature to which the sample has been exposed. Measurements of the temperature dependence of the ESR signal from the chars[17,18] also showed up electrical conductivity effects in some coals, particularly those heated above 400 °C in the flow cell at high sweep velocities of inert gas.[12-15] In agreement with previous work,[17] it was concluded that measurement of the temperature dependence of the ESR signal from pyrolysis chars is an essential procedure for determining the range of experimental variables over which assumptions inherent in the calculation of free-radical concentrations may be considered as valid.

b. The Curie law is derived by assuming a stable number of microwave-absorbing free radicals and relates the observed signal to the temperature of the sample. With the exception of anomalies detailed above,[15] all coals studied gave pyrolysis chars with temperature dependences of the ESR signal conforming to Curie law behavior. The implication must be that the free-radical population, developed during the pyrolysis of the sample on heating, reflects the presence of a constant number of free radicals and that these free radicals are stable over the temperature range (ambient to 500 °C in the present study) and the time (up to 1 h) during which Curie law conformity has been established. It was therefore concluded that the free radicals observed by ESR are the relatively stable product char free radicals. While these relatively stable free radicals have been observed to react slowly under further heat treatment,[19] they appear to have comparatively long lifetimes and not to act as reaction intermediates during pyrolytic devolatilization. This is the sense in which the term "stable free radical" will be used when referring to this class of free radicals in the remainder of this report.

c. Pyrolysis experiments performed at a slow heating rate (10 °C/min) between ambient temperature and 500 °C have allowed the identification of three distinct types of thermal processes on the basis of in situ spin population measurements during heatup.[10,15] The spin population, S, is defined here as free radicals per gram of initial sample mass, a definition that allows for the migration of volatiles out of the ESR-active zone during pyrolysis.

i. "Region 1": S rises to a relatively shallow maximum near 200 °C; this increase in signal arises from recovery of partial signal loss, through desorption of adsorbates such as oxygen[10,17] from both internal and external coal surfaces.

ii. "Region 2": S is observed to fall to a minimum in the vicinity of 300 °C. This fall of signal is attributed to thermally activated mobility of potentially mobile free radicals, enabling radical recombination reactions.

iii. "Region 3": S is observed to increase with increasing temperature. This increase is ascribed to the onset of bond thermolysis.

For some coals at temperatures above 400 °C, a second reduction in S is observed. This fall is always associated with an abnormal temperature dependence of the ESR signal[12-14] as a result of the electrical conductivity of the char in the microwave field.[17,18] The observed drop in S values at the higher temperatures thus appears to be an artifact of the technique, a conclusion confirmed by higher values of S being observed when the same char is removed from the cell, ground, and mixed with silica and a reading taken at room temperature.[12]

d. It was observed that increasing the sweep velocity of inert gas through the sample tube, in the flow cell, causes increases in the spin population beginning with the onset of region 3, before conductivity effects are observed.[12-15] Moreover, in a parallel series of experiments in a fixed-bed pyrolysis reactor,[13] it was shown that the tar yield and the tar structural parameters also change systematically with increasing gas sweep velocity. These results suggest that the rapid removal of pyrolysis tars from the reaction zone causes increases in the spin population by reducing the probability of recombination reactions between volatile tar molecules and the pyrolyzing char matrix.

On the basis of these ESR-based observations, it is possible to construct a conceptual model of the free-radical chemistry involved in the thermal reactions of coal.

Coal Pyrolysis Reactions from an ESR Perspective

All available information suggests that different types of free radicals exist in coal both before and during pyrolysis. In contrast to free radicals observable by ESR ("ESR-active": S•), there are also free radicals that are not detectable with electron spin resonance spectroscopy ("ESR-silent": R•).

There are several reasons why some free radicals are ESR-silent. First, if the free radical is very reactive, then its lifetime may be sufficiently short to broaden the line width such that the signal is no longer detectable.[10] Second, if the rate of creation of reactive free radicals is low and their lifetimes moderately short, then the population of the reactive free radicals at any given time may be insignificant compared with the background signal from "stable free radicals" (see below). Third, if the reactive free radicals are in the vapor phase, the line width will again broaden due to the coupling of the electronic spin and orbital angular momenta, which, for a polyatomic radical, leads to a multitude of undetectably weak lines.[20,21] It is noted that within this set of definitions, unheated coal is not expected to contain the R• type (i.e. ESR-silent) species.

(13) Gonenc, Z. S.; Fowler, T. G.; Kandiyoti, R.; Bartle, K. D. *Fuel* **1988**, *67*, 848.
(14) Fowler, T. G.; Kandiyoti, R.; Bartle, K. D.; Taylor, N. *Proc. Int. Conf. Coal Sci., 1987* **1987**, 617.
(15) Fowler, T. G.; Kandiyoti, R.; Bartle, K. D.; Snape, C. E. *Carbon* **1989**, *27*, 197.
(16) Stompel, Z.; Fowler, T. G.; Bartle, K. D. *Koks, Smola, Gaz* **1988**, *33*, 1356.
(17) Singer, L. S. *Proceedings of the Conference on Carbon, 5th, 1961*; Pergamon Press: New York, 1963; p 37.
(18) Retcofsky, H. L.; Hough, M. R.; Maguire, M. M.; Clarkson, R. B. *Appl. Spectrosc.* **1982**, *36*, 187.
(19) Singer, L. S.; Lewis, I. C. *Carbon* **1978**, *16*, 417.
(20) Wertz, J. E.; Bolton, J. R. *Electron Spin Resonance: Elementary Theory and Practical Applications*; McGraw-Hill: New York, 1972; p 345.
(21) Livingston, R.; Zeldes, H.; Conradi, M. S. *J. Am. Chem. Soc.* **1979**, *101*, 4312.

Both reactive and stable free radicals can be either mobile (m), or immobile (i). An immobile free radical is seen either as being bound to the coal macromolecular matrix or as a smaller molecular entity having a pore-diffusional activation energy not attainable at low temperatures. Moderate increases in temperature are expected to impart mobility to some of the latter type of free radicals.

At temperatures above 300 °C (region 3), greater numbers of free radicals are formed by covalent bond thermolysis; most new free radicals are thought to be mobile. Some initially trapped (immobile) free radicals are also rendered mobile by breaking open of occlusions. Thus the energetics of free-radical reactions is implicit in the above classification of stable (S•) and reactive (R•) free radicals. It is important, however, to recognize both kinetic and thermodynamic stability. Hence R• (i.e. ESR-silent) species are unstable both in the kinetic and the thermodynamic senses, whereas S• may or may not be thermodynamically stable. For example, some occluded free radicals may have long lifetimes (kinetic stability), due to their lack of mobility, despite being thermodynamically less stable than, e.g., free radicals associated with the polyaromatic ring systems of the coal matrix. In the following discussion, ESR-active yet inherently chemically reactive species will be denoted as S′•. Using these definitions, it is possible to suggest some general mechanisms for reactions during coal pyrolysis.

I. Region 1. Processes observable by ESR in this temperature range appear to be dominated by desorption effects. The ESR-spin population is observed to increase as partial loss of signal due to oxygen (and possibly water) adsorption is restored:[10,17]

$$J^{\bullet}O_2 \rightarrow J^{\bullet} + O_2(g) \tag{1}$$

where J• denotes $S_i^{\bullet}$, $S_i'^{\bullet}$, or $S_m^{\bullet}$.

II. Region 2. The drop in signal was concluded to be due to mobility-induced recombination reactions. It is thought that the extra mobility of free radicals can be due to the relaxation of the pore structure of the coal imparting mobility to trapped free radicals and/or the increased temperature imparting mobility to free radicals ($S_m^{\bullet}$ type) residing in initially nonclosed pores but themselves immobile at the lower temperatures.

$$S_i'^{\bullet} \text{ (or } S_i^{\bullet}) \rightarrow S_m'^{\bullet} \text{ (or } S_m^{\bullet}) \; (S_m'^{\bullet} = R^{\bullet}) \tag{2}$$

$$R_1^{\bullet} + R_2^{\bullet} \rightarrow (R_1{:}R_2)_{i \text{ or } m} \tag{3}$$

$$R^{\bullet} + J^{\bullet} \rightarrow (R{:}J)_{m \text{ or } i} \tag{4}$$

$$S_i'^{\bullet} + (R{:}H)_m \rightarrow (S'{:}H)_i + R^{\bullet} \tag{5}$$

$$J^{\bullet} + R^{\bullet} \rightarrow J_{m \text{ or } i} + (R{:}H)_m \tag{6}$$

$$(J{:}H) + R^{\bullet} \rightarrow (J^{\bullet})_{m \text{ or } i} + (R{:}H)_m \tag{7}$$

where J• has been defined above. The mobility imparted, by heating, to thermodynamically unstable radicals (eq 2) enables recombination reactions to take place (eq 3 and 4); some of the reactions covered by eq 4 allow for the possibility that the encounter of a thermodynamically unstable radical with S• may be sufficient to "force" a recombination. In reactions 6 and 7, the radical R•, created by H• abstraction by $S_i'^{\bullet}$ (eq 5), either recombines directly (as in eq 3 and 4) or abstracts a H• from a site adjacent to a stable free radical to yield a double bond (eq 6) or a relatively stable free radical (eq 7). Reactions 5–7 provide an example of hydrogen shuttling;[22] it is thought, however, that region 2 temperatures may be too low for the latter process to take place with any intensity but that in region 3 this may be an important mechanism for hydrogen transfer.

III. Region 3. Upon the onset of covalent bond-breaking reactions, the number of possible reaction types increases rapidly. Some of the more important may be classified as follows:

$$(J_1{:}J_2)_i \rightleftarrows J_1^{\bullet} + J_2^{\bullet} \tag{8}$$

$$(R_1{:}R_2)_{i \text{ or } m} \rightarrow R_1^{\bullet} + R_2^{\bullet} \tag{9}$$

$$(J{:}R)_i \rightarrow J^{\bullet} + R^{\bullet} \tag{10}$$

In region 3, recombination (eq 3, 4) and abstraction reactions (eq 5–7) would be expected to proceed at greater intensity than in region 2. Our previous work has shown that extents of recombination reactions can be altered by rapid removal of volatile products from the vicinity of the pyrolyzing coal matrix.[13]

On the Number of Broken Bonds: A Structural Model

The structure of coal is recognized to consist of cross-linked macromolecular structures, with smaller molecular units occluded within the pores. The macromolecular structures, and to a less extent the entrapped molecules, consist of aromatic units of about one to five (partially fused) ring structures, with associated side chains and hydroaromatic groups held together by bridging groups. In low-temperature pyrolysis, as in experiments cited,[9-16] the aromatic clusters are likely to survive intact. Thus, predominant reactions within the substrate matrix are thought to be confined to scission of bridging groups between aromatic clusters, scission of side chains, and functional group reactions, such as decarboxylation, the latter yielding mainly light gases. Simple topological arguments, confirmed by a model of coal pyrolysis (see below) suggest that the concentration of such bridging groups is of the order of (1–4) × 10^{21} groups/g. Furthermore, measurements of hydrogen uptake by Pittsburgh Seam coal during liquefaction indicate that, for complete conversion (to about 90% yield of soluble product), this coal requires about 1.4% of hydrogen by weight:[1] a number equivalent to 8.4 × 10^{21} hydrogen atoms/g of coal. That is, it appears that slightly more hydrogen is transferred to the coal than is required to cap both scission fragments of every bridging group in the coal. In practice, liquefaction with external addition of hydrogen is unlikely to reduce the molecular mass of every molecule in the product solution to 500 Da or less, as would be the case for the total breakdown of the coal model structure assumed in the above calculation. It appears therefore, that in such "complete hydrogenation" experiments the coal also accepts some hydrogen atoms at positions other than bridge scission sites.

While this is of interest, the main question under consideration is, how many bridging groups need to be broken in coal in order to release the observed yield of low molecular mass material (tars and gases) and is this number consistent with the increase in free-radical population observed by ESR? A topological computer model was built in an attempt to answer this question. This model in some respects resembles the model of Solomon et al.[23] A random series of molecular masses, which correspond with the basic aromatic units of the coal, was selected from a

(22) Neavel, R. C. *Fuel* **1976**, *55*, 237.

(23) Solomon, P. R.; Hamblen, D. G.; Deshparde, G. V.; Serio, M. A. *Proc. Int. Conf. Coal Sci., 1987* **1987**, 601.

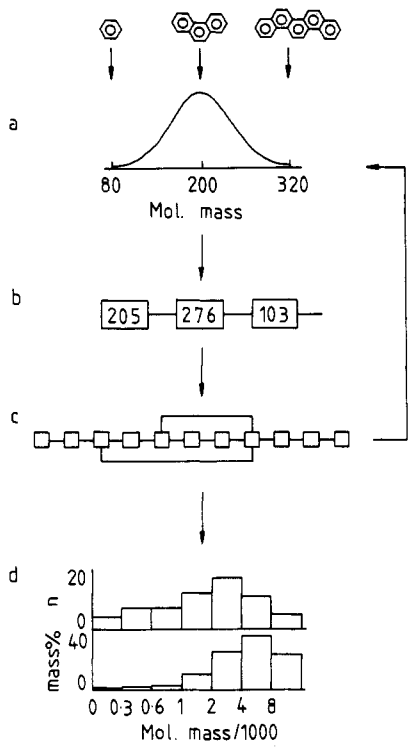

Figure 1. Generation of the topological coal model: (a) random molecular masses of basic units drawn from a Gaussian distribution; (b) basic units connected linearly by bridging groups (of assumed zero mass) until a termination criterion limits the chain length; (c) additional cross-links introduced at random, such that no fragment is linked to others by more than four bridges with steps a–c repeated until about 60 macro-molecules are generated; (d) number and mass percent distributions and other characteristic parameters of the model calculated.

Gaussian distribution until a termination probability condition (defining the size of the current cluster or macromolecule) was satisfied (Figure 1). The parameters defining the Gaussian curve were chosen such that the mean molecular mass of individual clusters within the coal molecules corresponds with that of a typical substituted anthracene, the wings of the distribution extending to cover molecular masses between one and five fused aromatic rings. An adjustable number of cross-link bridges (linking the basic aromatic units) was then entered at random within the current macromolecule, such that no more than four bridging groups were attached to any one basic unit.[24] This process was continued until about 60 coal macromolecules had been generated. Simple adjustment of the termination criteria effectively determines the initial molecular mass of the generated model molecules.

The structural parameters of the model, such as the number and mass average molecular mass, the number of bridging groups per gram, and the molecular mass distribution were then calculated. Pyrolytic reactions were then simulated as follows: bridging groups were progressively broken at random and new structural parameters calculated each time a distinct new molecular entity had been created as the result of breaking a bridging group. The model is schematically outlined in Figure 2 and typical results of these calculations are shown in Table I.

From Figure 2d, it can be seen that simulated pyrolysis has little effect on the mass percent distribution as would be expected when over 80% of the product is char. In

Table I. Results of Computer Model Pyrolyses

model		tot. no. of bridges in model	cross-link density[a]	density of bridges[b]/ 10^{21} g^{-1}	max generated free-radical density[c]/ 10^{19} g^{-1}	calcd yield/%		M_n	M_w	molecular mass distribn/% of tot.					
coal	char					extract[d]	tar[e]			0–300 Da	301–600 Da	601–1000 Da	1001–2000 Da	2001–4000 Da	4001–8000 Da	8000 Da+
1		876	0	2.86	0	2.3		3180	6930	0.3	3.2	1.7	8.6	17.2	28.4	40.6
	1	856		2.80	13.1		8.6	2360	4670	1.1	2.9	2.4	13.1	24.4	40.8	15.3
2		850	0	2.77	0	2.3		2600	5160	1.0	0.8	3.4	13.6	33.1	25.6	22.6
	2	834		2.72	10.4		9.4	2120	3910	1.2	1.8	4.1	16.9	45.9	20.6	9.5
3		855	0	2.80	0	1.8		2710	4660	0.9	1.2	2.0	8.8	38.8	32.7	15.6
	3	835		2.73	13.1		9.6	2090	4110	1.7	2.3	3.1	12.8	37.1	32.5	10.4
4		1004	0.14	3.25	0	2.0		3260	10400	0.1	2.7	1.7	12.3	17.6	26.0	39.6
	4	959		3.10	29.1		9.9	2550	9930	1.0	4.4	2.1	14.2	16.6	22.8	39.0
5		978	0.12	3.18	0	1.7		3140	5600	0.3	1.1	2.5	11.4	19.8	37.8	27.0
	5	924		3.00	35.1		9.9	2340	4880	0.8	2.8	3.8	14.2	23.0	33.9	21.4
6		971	0.12	3.19	0	2.4		2910	5090	0.5	1.8	3.0	10.4	25.4	35.9	23.0
	6	942		3.10	19.1		10.0	2440	4840	1.0	2.8	3.7	12.2	25.3	32.3	22.8

[a] Cross-link density = number of cross-link bridges/(total number of bridges − number of cross-link bridges). [b] Density of bridges = total number of bridges/total mass of model. [c] Maximum free-radical density = 2 × number of broken bridges/total mass of model. [d] Extract yield = 4(sub-1000 mass fraction)/9. [e] Tar yield = 4(sub-1000 mass fraction)/3.

(24) Niksa, S.; Kerstein, A. R. *Proc. Int. Conf. Coal Sci., 1987* **1987**, 593.

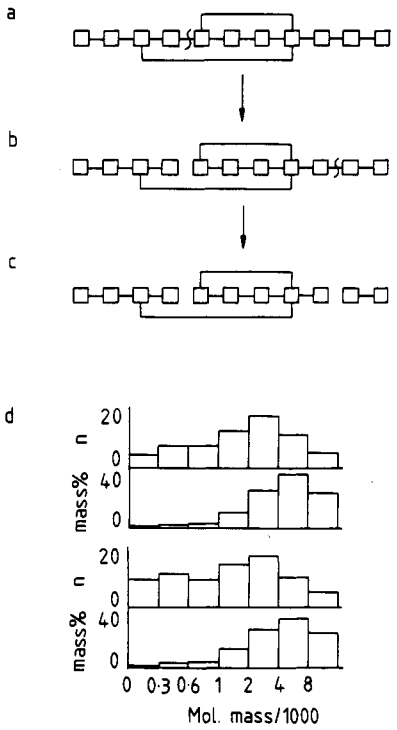

Figure 2. Simulation of pyrolysis using the topological model: (a) typical coal molecule showing site for broken bridge, picked at random; (b) second scission leading to lighter fragment, unlike first scission; (c) net result of the two bond scissions; (d) effect of pyrolysis to a 10% tar yield (as defined in the text) on the number and mass percent distribution of the model (lower graph), compared with the original model (upper graph). Total model includes light tar and gas.

contrast, in the number distribution there is a pronounced shift to low molecular mass consistent with the release of pyrolysis tars and vapors.

Previous experimental work[13,25] has shown that about 75% of the yield of chloroform (Soxhlet) extracted material or slow pyrolysis tar is in the sub-1000 molecular mass range. It is likely that Soxhlet extraction with chloroform leaves an appreciable quantity of low molecular mass material still occluded within the coal mass after extraction. To simulate this, it is assumed that one-third of the sub-1000 molecular mass fraction of the coal model is equal to 75% of the experimental value of the chloroform (Soxhlet) extraction yield. The model extraction yield of nonpyrolyzed coal is thus calculated as

model extract yield =
(4/9)(sub-1000 mass fraction of coal model) (11)

However, during pyrolysis (after some model bridges have been broken) more complete recovery of the total obtainable low molecular mass material is expected (partly intact originally occluded material, plus partially reacted–dealkylated etc. originally occluded material, plus low molecular mass material formed through pyrolytic fragmentation), due to the combined effects of bond thermolysis and because much of the pore structure has been opened up. Therefore, the total sub-1000 molecular mass fraction of the simulated solid substrate (after some bridges in the model have been broken) is equated to 75% of the experimental slow pyrolysis tar yield, as follows:

model tar yield =
(4/3)(sub-1000 mass fraction of model) (12)

The assumptions inherent in eq 11 and 12 are made only in order to estimate the number of homolytic bond scissions and are derived from extraction and pyrolysis tar yield data obtained with Linby coal. From these assumptions, it can be seen that the initial states of the models shown in Table I are not unreasonable representations of the molecular structure of Linby coal, as the chloroform extract yield of Linby coal has been measured to be about 2%.[25] This chloroform extract yield would imply that the total sub-1000 Da content of Linby coal should be about 4.5%. In recent experiments,[26] the extraction of Linby coal with tetrahydrofuran gave a 14% yield, about 35% of this material—i.e. 4.9% of the daf original coal—being found by size-exclusion chromatography to be below 1000 Da. Thus, for Linby coal, even assuming no adduction of THF to extracted materials, 4.9% seems reasonably close to the estimate based on assumptions underlying eq 11.

From Table I, it is apparent that, even for macromolecular structures without any cross-links (models 1–3), the maximum generated free-radical density rises to a value well *in excess of* that inferred from ESR measurements ((4–6) × 10^{19} free radicals/g) as the experimentally observed minimum tar yield[13] (10%) under comparable conditions is approached. Clearly, when cross-linked models are considered (models 4–6 in Table I), this discrepancy between calculation and observation increases dramatically, despite the use of open structures in agreement with experimental estimates of cross-link densities of about 1 cross-link/1500 Da.[27] It follows from this reasoning, which contains some apparently reasonable assumptions, that the observed tar yields can be made to agree with ESR-derived free-radical densities only by accepting that the free radicals observed by ESR represent a comparatively small, and probably relatively unreactive, fraction of the total number of free radicals formed during low-temperature pyrolysis. It would appear therefore that attempts at linking ESR-derived free-radical densities to coal reactivity would be based on incorrect assumptions.

It should be noted that the effects of repolymerization have been neglected in the above model. However, this is not considered to be critical in the present context because recombination will reduce both the tar yield and the free-radical concentration, thus requiring more primary reactions to reach the experimental tar yield. The consequences of recombination reactions will be considered explicitly in the next section.

Some Kinetic Considerations Pertinent to Coal Pyrolysis

Implicit in the above discussion is our acceptance of the general consensus on the mechanisms of coal pyrolysis. That is, pyrolysis is initiated by a set of parallel first-order (relatively slow) reactions that yield free-radical intermediates. These intermediates then participate in a cascade of (probably faster) secondary reactions. This reaction cascade, which is of variable and unknown length, is terminated when the intermediates finally react to form relatively stable products. It should be obvious from the foregoing that our understanding of the initial ("static") coal structure is by no means complete. Furthermore, any estimate of the concentration of free-radical intermediates generated during pyrolysis will rely on ill-defined kinetic parameters. Nevertheless, the estimate of the concentra-

(25) Neuburg, H. J.; Kandiyoti, R.; O'Brien, R. J.; Fowler, T. G.; Bartle, K. D. *Fuel* **1987**, *66*, 486.

(26) Gonenc, Z. S. Ph.D. Thesis, University of London, in preparation.

(27) Larsen, J. W.; Green, T. K.; Chiri, I. *Proc.–Int. Conf. Coal Sci., 1983* **1983**, 277.

Table II. Free-Radical Intermediate Concentration Calculated from Eq 16–18[a]

		U_1/free radicals g^{-1}			U_2/free radicals g^{-1}		
t/min	R/free radicals g^{-1} s^{-1} [b]	$k_1 = 0.01$	$k_1 = 1.0$	$k_1 = 100$	$k_2 = 10^{-4}$	$k_2 = 10^{-17}$	$k_2 = 10^{-20}$
2	8.3×10^{18}	8.3×10^{20}	8.3×10^{18}	8.3×10^{16}	2.9×10^{16}	9.1×10^{17}	2.9×10^{19}
10	1.7×10^{18}	1.7×10^{20}	1.7×10^{18}	1.7×10^{16}	1.3×10^{16}	4.1×10^{17}	1.3×10^{19}
20	8.3×10^{17}	8.3×10^{19}	8.3×10^{17}	8.3×10^{15}	9.1×10^{15}	2.9×10^{17}	9.1×10^{18}

	U_3/free radicals g^{-1} (for $R = 8.3 \times 10^{18}$ free radicals g^{-1} s^{-1})								
	$C = 10^{18}$ g^{-1}			$C = 10^{20}$ g^{-1}			$C = 10^{21}$ g^{-1}		
k_3	$k_2 = 10^{-14}$	$k_2 = 10^{-17}$	$k_2 = 10^{-20}$	$k_2 = 10^{-14}$	$k_2 = 10^{-17}$	$k_2 = 10^{-20}$	$k_2 = 10^{-14}$	$k_2 = 10^{-17}$	$k_2 = 10^{-20}$
10^{-16}	2.4×10^{16}	8.3×10^{17}	8.4×10^{16}	8.3×10^{14}	8.4×10^{14}	3.6×10^{16}	8.3×10^{13}	5.6×10^{14}	0
10^{-18}	2.9×10^{16}	8.6×10^{17}	7.7×10^{18}	2.4×10^{16}	8.3×10^{16}	8.3×10^{16}	7.7×10^{15}	8.3×10^{15}	1.4×10^{16}
10^{-20}	2.9×10^{16}	9.1×10^{17}	2.8×10^{19}	2.9×10^{16}	8.6×10^{17}	7.7×10^{18}	2.8×10^{16}	5.4×10^{17}	8.3×10^{17}

[a] Units of k_2 and k_3 are g (free radical)$^{-1}$ s^{-1}; units of k_1 are s^{-1}. [b] $R = 10^{21}/(60t)$.

tion of free-radical intermediates is instructive and will now be addressed.

In the previous section, it was concluded, from structural considerations alone, that the signal observed by in situ ESR is at least mainly associated with relatively stable product free radicals, rather than the more reactive free-radical intermediates. The concentration of reactive free-radical intermediates during pyrolysis will now be estimated for various experimental conditions by using assumptions that *maximize* the probability of observing the intermediates against the stable free-radical background. The assumption that is most likely to overestimate the expected ESR signal (and to be invalid) is that *all* reactive free-radical intermediates formed by thermolysis are observed by ESR. That is, lifetime broadening is not significant, vapor-phase radicals do not form, and no free radicals escape the ESR-active zone. In the previous section, it was concluded that the concentration of bridging groups that need to be broken to release the observed yield of tar was about 10^{20} groups/g. This represents only about 3% of the initial number of bridging groups. Here it is assumed that 5×10^{20} bridging groups/g break during low-temperature pyrolysis, which releases a total of 10^{21} free radicals g^{-1} as the yield of primary pyrolysis reactions. The concentration of free-radical intermediates at any time, t, depends both on the time dependence of the rate of release of primary pyrolysis reaction products, $P(t)$, and on the mechanism(s) whereby the intermediates react to form stable products, as opposed to other intermediates. (N.B. The integral

$$\int_0^\infty P(t)\, dt$$

is defined above as 10^{21} free radicals/g.) Three cases will be considered. First, the decay kinetics may be effectively first order because the free-radical intermediates are stabilized by reaction with functional groups on the coal macromolecule that are assumed to be in large excess. Equation 13 describes such a situation, where $U(t)$ is the

$$\frac{dU(t)}{dt} = P(t) - k_1 U(t) \qquad (13)$$

concentration of free-radical intermediates at any time and k_1 is the mean first-order rate constant for the formation of stable product species. (Note that U-type radicals are likely to correspond with the R$^\bullet$ species described above.) Second, at the other extreme, free-radical intermediates may be stabilized only by reaction with each other, in which case eq 14 is appropriate, where k_2 is the mean

$$\frac{dU(t)}{dt} = P(t) - k_2[U(t)]^2 \qquad (14)$$

second-order rate constant for radical–radical recombination reactions. Third, a superposition of these two mechanisms may be more realistic as both direct recombination and reaction with the coal macromolecule seem reasonable reaction mechanisms.

$$\frac{dU(t)}{dt} = P(t) - k_3 C(t)\, U(t) - k_2[U(t)]^2 \qquad (15)$$

where $C(t)$ is now (in contrast to the assumption underlying eq 13) an adjustable concentration term that decreases as the stabilizing functional groups on the coal macromolecule are consumed and k_3 is the mean rate constant for these reactions.

In order to evaluate $U(t)$, either analytically or numerically, it is first necessary to estimate values for k_i and $C(t)$. Estimation of rate constants for coal pyrolysis reactions can be approached from two directions, although neither will prove wholly satisfactory. Much work has been performed to fit experimental weight loss curves to various kinetic models (e.g. ref 4). To obtain reasonable agreement with a first-order model, it is necessary to use a minimum of two activation energies; the first to model the initial rapid devolatilization and the second to characterize the slower weight loss taking place at longer times spent at peak temperature. Clearly, weight loss is a rather gross variable to attempt to fit, since a multiplicity of processes influence the final result. For example, the breaking of any one bridge does not guarantee a contribution to the observed weight loss. Despite this limitation, it is interesting to note that kinetic parameters obtained by fitting weight loss data[4] broadly agree with those obtained by fitting the rise in ESR-spin population for "rapid" heating experiments.[28] Again, at least two activation energies are required for a sufficient agreement with experimental values. The rate constants obtained during the present study from rapid-pyrolysis ESR experiments at 450 °C are about 0.01 and 0.002 s^{-1} for a first-order fit. We would view the near coincidence of ESR-derived kinetic parameters with weight loss data as further evidence that the free radicals observed by ESR are product free radicals, not intermediates, because they appear at about the same rate as the occurrence of "weight loss", the latter term denoting a reaction product by definition. The values quoted above (i.e. 0.01–0.002 s^{-1} for the devolatilization stage) represent our lower estimate for the value of k_1.

The second approach to evaluation of coal pyrolysis kinetic parameters is to estimate the rates of the elementary reaction steps.[4] Such estimates are about equally difficult to relate to macroscopic quantities, as again there is no tangible one-to-one relationship between the molecular scale and observable events. Furthermore, trans-

(28) Fowler, T. G.; Bartle, K. D.; Kandiyoti, R. *Fuel* **1988**, *67*, 1249.

port-related processes are likely to have a significant influence on the results: the latter are probably more complicated to evaluate than chemical kinetics. Bearing in mind these reservations, the values quoted in ref 4 lead to rate constants at 450 °C of 4×10^{-13} g (free radical)$^{-1}$ s^{-1} for recombination reactions (i.e. k_2) and between 3×10^{-12} and 1×10^{-18} g (free radical)$^{-1}$ s^{-1} for hydrogen abstraction reactions, which are likely to be the major reaction pathway with the coal macromolecule (i.e. k_3) again at 450 °C.

These calculated values represent our upper estimates for k_2 and k_3; in practice, the values are likely to be reduced through mass-transport limitations. The initial value of $C(t)$ can be estimated from the hydrogen content of the coal or char, as it is assumed that the major reaction that is associated with the term k_3 is hydrogen abstraction from the coal macromolecule by a free-radical intermediate. Low-temperature chars (pyrolyzed to 500 °C) contain about 3% hydrogen by weight,[12] which translates to about 2×10^{22} hydrogen atoms/g. Assuming 1–10% of these to be abstractable yields an initial value of $C(t)$ between 10^{20} and 10^{21} g^{-1}. Using the range of values deduced above and making two further assumptions, namely that $P(t)$ and $C(t)$ are both constant, it is possible to solve eq 13–15 analytically (eq 16–18) and to calculate some equilibrium values

$$U_1 = (P/k_1)[1 - \exp(-k_1 t)] \tag{16}$$

$$U_2 = a\frac{1 - \exp(-2ak_2 t)}{1 + \exp(-2ak_2 t)}; \qquad a^2 = P/k_2 \tag{17}$$

$$U_3 = b\frac{k_3 C[1 + \exp(-2bk_2 t)] + 2bk_2[1 - \exp(-2bk_2 t)]}{k_3 C[1 - \exp(-2bk_2 t)] + 2bk_2[1 + \exp(-2bk_2 t)]} - \frac{k_3 C}{2k_2} \tag{18}$$

$$b^2 = \frac{(k_3 C)^2}{4(k_2)^2} + \frac{P}{k_2}$$

for $U(t)$, which are shown in Table II. It should be noted that the equilibrium concentrations of free-radical intermediates shown in Table II agree within 10% with simple numerical summation solutions of eq 13–15. In addition, these numerical solutions also indicate that the results in Table II are not significantly different when time-dependent values of $P(t)$ and $C(t)$ are allowed. Comparison of the equilibrium concentration of free-radical intermediates (U_1) calculated from eq 16 with those calculated from eq 17 and 18 (U_2 and U_3) immediately indicate that the first-order rate parameters, deduced by fitting weight loss data, give rise to intermediates with much longer lifetimes compared with those resulting from the second-order decay constants. This large difference is probably at least partly a consequence of the fact that it is tacitly assumed in the estimate of k_2 and k_3 above that the product of *every* elementary reaction is a nonreacting product species. However, it is possible to imagine a large number of elementary reactions taking place during coal pyrolysis that contribute little (directly) to the overall reactivity or distribution of products observed, but has the effect of limiting the lifetime of any one intermediate species. For example, a reactive free radical will have little difficulty in abstracting a hydrogen atom from any convenient source, but the result may well be a free radical almost as reactive as the one destroyed, and so no stable product has been produced. Thus the effective values of k_2 and k_3 are reduced not only by resistances to mass transfer but also by a factor determined by the average number of reaction steps between formation and decay of the free-radical intermediate. Unfortunately, it is not possible to even guess at these quantities within our relatively simple model.

During coal pyrolysis, ESR measures a spin population of about $(1–5) \times 10^{19}$ g^{-1}. Thus in order to observe free-radical intermediates with ESR against this background signal, the concentration of the intermediates must rise to at least 5% of the measured ("background") figure, and this figure (i.e. 5%) must be maintained for at least 30 s, judging from the performance of our spectrometer. Although there is nothing unique about these figures, it does seem clear that an intermediate free-radical concentration of at least 10^{18} g^{-1} must be achieved if reactive free-radical intermediates are to be observed by ESR during coal pyrolysis. From Table II, this criterion is met for the smaller values k_1–k_3 for each functional form of the equations by using, it must be stressed, assumptions that maximize the probability of "observing" free-radical intermediates (e.g. that five times more radicals are released than our calculations indicate are necessary over a time interval of down to 2 min and that all free radicals released are observed). The physical significance of the parameters selected will now be discussed, taking the results from eq 13–15 in turn.

An observable free-radical intermediate concentration can be calculated from eq 13 provided $k_1 \leq 1$ s^{-1} and pyrolysis reactions are complete in less than 10 min. For first-order decay kinetics, the mean lifetime is given by ln $(2/k_1)$. Therefore, to observe an ESR signal from intermediate lifetime free radicals, their lifetime from formation to removal (i.e. after accounting for multiple reaction steps), must exceed 0.7 s. While this may be possible, provided the number of elementary steps between formation and product is large, the large concentration of free-radical intermediates so obtained would indicate that it is incorrect to neglect a second-order radical recombination term in eq 13. In addition, our estimate of the order of magnitude of $C(t)$ for eq 15 would indicate that it is incorrect to assume a large concentration excess of functional groups on the coal macromolecule that are able to participate in termination reactions. That is, as U_1 increases, the functional form of eq 13 becomes less acceptable.

For eq 14 and 15, an observable concentration of free-radical intermediates is only obtained if k_2 is less than 10^{-17} g (free radical)$^{-1}$ s^{-1}. This is at least 4 orders of magnitude slower than the rate constants estimated in ref 4. Similarly, for eq 15, k_3 must be smaller than estimates of hydrogen abstraction rate constants estimated in ref 4, and C must be less than or equal to 1% of the total hydrogen content of the char.

In addition, it may not be a coincidence that the concentration of free radicals, which decay via the $k_3C(t)\ U(t)$ term in eq 15, is often of the same order of magnitude as the rise in free-radical concentration observed by ESR. The significance of this is made clear when it is understood that the k_2 and k_3 terms in eq 15 correspond respectively with

$$\mathrm{U^{\bullet} + U^{\bullet} \rightarrow U{:}U} \tag{19}$$

$$\mathrm{U^{\bullet} + (coal{:}H) \rightarrow (U{:}H) + coal^{\bullet}} \tag{20}$$

Thus the conclusion from this section is that free-radical intermediates could be observed by in situ ESR under favorable conditions of rapid heating, provided the number of elementary reaction steps between formation and decay is large and/or the recombination rate constants are significantly smaller than indicated.[4] However, we believe these conditions are unlikely to be satisfied for the majority of coals, and therefore, free-radical intermediates are, in

general, ESR silent in agreement with conclusions drawn from experimental results.[9-16]

Conclusions

1. In situ ESR studies of coal pyrolysis are explained by a conceptual model of coal reactivity. The wide variety of ESR concentration profiles obtained from coals is the result of a complex interplay between mobile and immobile free-radical species that are relatively stable (ESR observable) or reactive (ESR silent).

2. A simple topological model of coal structure indicates that more free radicals must be created during coal pyrolysis in order to release the observed yield of tar than are observed by in situ ESR. The implication is that many of the free radicals created by pyrolysis must be ESR silent.

3. The weight of evidence from kinetic calculations of the concentration of free-radical intermediates formed during pyrolysis confirm that the concentration of reactive free-radical intermediates is small compared with that from stable product free radicals. The observation of reactive coal free-radical intermediates with in situ ESR during thermal treatment, therefore, appears unlikely and remains to be demonstrated.

Acknowledgment. We express our thanks to British Coal (CRE) for the supply of samples and the U.K. Science and Engineering Research Council for support under Research Grant GR/D/03581.

Activation Energy of Air-Oxidized Bituminous Coals

Mollie L. E. TeVrucht and Peter R. Griffiths*

Department of Chemistry, University of California, Riverside, California 92521

Received April 6, 1989. Revised Manuscript Received May 22, 1989

The kinetics of air oxidation of a series of bituminous coals were investigated by using diffuse reflectance Fourier transform infrared spectrometry. A low-volatile bituminous coal, a medium-volatile bituminous coal, and two high-volatile A bituminous coals were ground to three particle sizes and oxidized at 150, 200, and 250 °C. Activation energies and rate constants for the air oxidation of these coals were determined by tracking the decrease in the intensity of the aliphatic C–H band centered near 2920 cm^{-1}. The air oxidation is found to obey pseudo-first-order reaction kinetics if oxygen is present in unlimited supply. The rate of oxidation was found to depend on particle size, rank, and temperature but to be independent of geographic origin and mineral content for the coals studied. Activation energies were calculated to be between 25.6 and 26.6 kcal/mol.

Introduction

Oxidation has a number of important effects upon the chemical and physical properties of coal. It can alter the coal's coking properties, the amount of extractable material available from the coal, and the tar yield of the coal.[1,2] The effects of oxidation have been studied by using a variety of analytical techniques including Mössbauer spectroscopy,[3] Audibert–Arnu dilatometry,[4] Gieseler plastometry,[3,4] X-ray photoelectron spectroscopy (XPS),[3,4] fluorescence spectroscopy,[5] and infrared spectrometry.[3-17]

Although the effect of oxidation upon coal properties has been well characterized, the kinetics and mechanism of oxidation are not fully understood. It is not known which step in the oxidation is the rate-limiting one. If oxidation is diffusion-controlled, a coal that is finely ground will oxidize more quickly because of its higher surface area to volume ratio. However, if some other reaction step limits the rate of oxidation, all particle sizes should oxidize at an equal rate.

The parameter of particle size has been investigated by several researchers, with conflicting results. In a study of oxidized coal using photoacoustic Fourier transform infrared spectrometry, McClelland and co-workers found that coal particles (44–125 μm) appeared to oxidize uniformly rather than to a decreasing degree with depth.[13] Their results imply that the rate of oxidation is not diffusion-limited. Carpenter and Sargeant determined that coal crushed to 50–100-μm particles had an oxidation rate independent of particle size.[18] Using much larger particles

(1) Berkowitz, N. *An Introduction to Coal Technology*; Academic Press: New York, 1979; pp 95–105.
(2) Gray, R. J.; Rhoades, A. H.; King, D. L. *Trans. Soc. Min. Eng. AIME* **1976**, *260*, 334.
(3) Huffman, G. P.; Huggins, F. E.; Dunmyre, G. R.; Pignocco, A. J.; Lin, M.-C. *Fuel* **1985**, *64*, 849.
(4) Wu, M. M.; Robbins, G. A.; Winschel, R. A.; Burke, F. P. *Energy Fuels* **1988**, *2*, 150.
(5) Kister, J.; Guiliano, M.; Mille, G.; Dou, H. *Prepr. Pap.—Am. Chem. Soc., Div. Fuel Chem.* **1987**, *32*, 21.
(6) Donini, J. C.; LaCour, S. A.; Lynch, B. M.; Simon, A. *Coal: Phoenix '80s. Proc. CIC Coal Symp., 64th, 1981*, **1981**, *1*, 132.
(7) Kister, J.; Mille, G.; Dou, H. *C. R. Acad. Sci., Ser. 2* **1986**, *302*, 621.
(8) Gethner, J. S. *Appl. Spectrosc.* **1987**, *41*, 50.
(9) Gethner, J. S. *Fuel* **1987**, *66*, 1091.
(10) Rhoads, C. A.; Senftle, J. T.; Coleman, M. M.; Davis, A.; Painter, P. C. *Fuel* **1983**, *62*, 1387.
(11) Lynch, B. M.; Lancaster, L.-I.; MacPhee, J. A. *Energy Fuels* **1988**, *2*, 13.
(12) Fredericks, P. M.; Moxon, N. T. *Fuel* **1986**, *65*, 1531.
(13) Chien, P.-L.; Markuszewski, R.; McClelland, J. F. *Prepr. Pap.—Am. Chem. Soc., Div. Fuel Chem.* **1985**, *30*, 13.
(14) Fuller, M. P.; Hamadeh, I. M.; Griffiths, P. R.; Lowenhaupt, D. E. *Fuel* **1982**, *61*, 529.
(15) Griffiths, P. R.; Wang, S.-H.; Hamadeh, I. M.; Yang, P. W.; Henry, D. E. *Prepr. Pap.—Am. Chem. Soc., Div. Fuel Chem.* **1983**, *28*, 27.
(16) Smyrl, N. R.; Fuller, E. L., Jr. In *Coal and Coal Products: Analytical Characterization Techniques*; Fuller, E. L., Jr., Ed.; ACS Symposium Series 205; American Chemical Society: Washington, DC, 1982; p 133.
(17) Fuller, E. L., Jr.; Smyrl, N. R. *Fuel* **1985**, *64*, 1143.
(18) Carpenter, D. L.; Sargeant, G. D. *Fuel* **1966**, *45*, 311.

0887-0624/89/2503-0522$01.50/0